

DESIGN CONSTRAINTS FOR e^+e^- SUPERCOLLIDERS
 AT ENERGIES OF 0.5-2.0 TeV PER LINAC*

 D. Chernin
 A. Mondelli

 Science Applications International Corporation
 1710 Goodridge Drive
 Mc Lean, VA 22102

Summary

There is a large gap in parameters between the design point for the SLC, and the next generation of linear supercolliders, whose center-of-mass (CM) energy per elementary constituent ($\sim 1-4$ TeV) will rival that of the SSC. This paper explores the constraints on the linear supercollider, based on scaling SLC technology, for 0.5, 1.0, and 2.0 TeV linacs.

An earlier study¹ has explored the frequency scaling for the linear supercollider, and concluded that x-band (or higher) frequencies would be advantageous. The power consumption of a linear supercollider has been studied in a recent report², which demonstrates that a 0.5 TeV-0.5 TeV linear supercollider with average ac power consumption of 50 MW/linac can be built using SLC technology, but concludes that high average accelerating gradient will lead to an inefficient accelerator with correspondingly high average power requirements. A good trade-off between gradient and power consumption appears to occur around 80 MeV/m.

The step from the SLC to a 0.5 TeV-0.5 TeV collider already contains many of the features required for colliders having 1 or 2 TeV per linac. In a 0.5 TeV linac the use of multiple (≈ 10) electron and positron bunches per rf pulse is essential if the accelerator efficiency is to be maintained at a reasonable value. This requirement leads to complications in damping ring design, multi-bunch wake field effects in the linacs, and problems with debris at the interaction point. All of these issues must be overcome in the 0.5 TeV-0.5 TeV collider. Quantitatively, of course, they become worse at higher energy.

The role of beamstrahlung is also very different at 0.5 TeV than at SLC. In the SLC the fraction of the beam energy radiated will be very small, and the radiation will be entirely classical. At 0.5 TeV, the beamstrahlung will be a dominating factor for the beam dynamics in the final focus; as much as 30% of the available beam energy may be lost. Also, the radiation spectrum will show significant quantum effects, entering a "transition regime"³ that is neither classical nor deep-quantum beamstrahlung. At higher energies, the fraction of the beam energy lost to beamstrahlung must not increase because the associated intrabunch energy spread would become intolerable.

Above 1 TeV per linac, the conservative design approach which we have pursued becomes very difficult to carry out. New structures to deal with wake fields, flat beams, elliptical irises, and new methods for power conditioning and pulse compression all seem necessary. In addition, the interaction-point scaling looks extremely difficult at 2 TeV, primarily because of the requirement that the luminosity scale as the square of the CM energy; operating windows in parameter space are found only after relaxing this requirement.

Interaction-Point Parameter Scaling

We will assume that the electron and positron bunches which collide at the interaction point (I.P.) are symmetric, that is, they have the same energy, number of particles per bunch, size and (Gaussian) shape; we will also assume that the bunches collide 'head-on.' Under these conditions the interaction may be characterized by ten quantities, viz. energy ($m\gamma c^2$), total luminosity (L_T), number of particles per bunch (N), bunch aspect ratio (R), (smaller) bunch transverse dimension (σ_y), bunch length (σ_z), average bunch collision rate (ν), disruption parameter (D), average beam power (P_b) and the fractional energy loss to beamstrahlung (δ_{BS}). These are related by

$$L_T = \frac{\nu N^2 H_D}{4\pi R \sigma_y^2} \quad (1)$$

$$\delta_{BS} = \frac{2}{3} \frac{r_e^3 N^2 \gamma H_D H_\delta}{\sigma_y^2 \sigma_z} \frac{F(R)}{R} \quad (2)$$

$$D = \frac{2r_e N \sigma_z}{(1+R)\gamma \sigma_y^2} \quad (3)$$

$$P_b = \nu N m \gamma c^2 \quad (4)$$

where r_e = classical electron radius. The quantities H_D (D , R) and H_δ , the pinch enhancement factor and the quantum mechanical correction to beamstrahlung, are defined in [1].

Of the ten I.P. quantities two, the particle energy and the luminosity, are typically specified early in the design process. If, in addition, we consider specifying R then the four relations among the seven remaining quantities give a three dimensional parameter space which we can display in slices. We have chosen to 'slice' this space by a $\sigma_x - \sigma_y$ plane of fixed P_b . In that plane we may plot curves of constraint for the remaining four quantities (N , ν , D , and δ_{BS}), using our best estimates as to what maximum acceptable values for these quantities would be. Depending upon our choices, a region in the plane - an operating window simultaneously satisfying all constraints - may emerge.³

An example from reference 2 is shown in Figure 1. The parameters for this figure are $m\gamma c^2 = 0.5$ TeV, $L = 10^{33}$ /cm² /s, $R = 1$, and $P_b = 0.5$ MW. The curves of constraint are $N_{max} = 5 \times 10^{10}$, $\nu_{max} = 3$ kHz, $D_{max} = 3$, and $\delta_{BS,max} = 0.3$. The operating window is shown shaded in the figure. Point A of Figure 1 is used for the accelerator parameter study at 0.5 TeV, below.

Once an operating window has been established at 0.5 TeV one may reasonably ask which parameters need to be 'pressed' in order to obtain a window at 1.0 TeV. For example, if we simply retain the same values of the constraints on N , ν , D , and δ_{BS} as at 0.5 TeV and try to increase the energy to 1.0 TeV, while simultaneously increasing the luminosity to 4×10^{33} cm⁻² s⁻¹ in the $P_b = 0.5$ MW plane, the window closes completely; in particular it becomes impossible to satisfy the constraint on D . Increasing the beam power to 1 or even 2 MW still does not open a window in the corresponding planes. If, however, one increases the rep rate (ν) constraint to $\nu_{max} = 10$ kHz then a very small window does open in the $P_b = 1$ MW plane, as shown in Figure 2. The point is that, under the constraints we have chosen, one must 'buy' luminosity with rep-rate.

This conclusion may be shown analytically by manipulating Eqs.(1-4). The upper right hand corner of the window, for example, determined by fixing $D = D_{max}$ and $\delta_{BS} = \delta_{BS,max}$, may be calculated in the approximation that³ $\Upsilon H_\delta \approx 1/6$ (intermediate beamstrahlung regime), which is applicable to our parameters. One finds

$$\sigma_x = \frac{D H_D P_b}{4\pi m c^2 r_e L_T} \quad (5)$$

$$\nu = \frac{4\pi}{H_D} \left(\frac{4\alpha r_e}{27\delta_{BS}} \right)^2 L_T \quad (6)$$

$$N = \frac{P_b}{\nu m \gamma c^2} \quad (7)$$

$$\sigma_y = \frac{4\alpha N r_e}{27\delta_{BS}} \quad (8)$$

where α is the fine structure constant.

We note in particular that if we demand $L_T \sim \gamma^2$ then $\mu \sim \gamma^2$ and $N \sim \gamma^{-3}$, for fixed beam power; if we allow $P_b \sim \gamma$, then $N \sim \gamma^{-2}$.

The scaling of rep-rate with luminosity would seem to place severe (~ 40 kHz) requirements on the rep-rate for a 2×2 TeV collider with a luminosity of four times that of the 1 TeV case. If instead we agree to consider the 2×2 TeV case with the same luminosity but double the beam power of the 1×1 TeV machine, then one sees from Eqs. (5-8) that ν , N , and σ_y remain fixed while σ_x just doubles. Figure 3 illustrates this case; the small window at 1 TeV has simply been displaced in σ_x .

Accelerator Parameter Studies

A detailed model for a SLAC-like rf linac has been developed¹⁻² and exercised to determine allowed regions on a parameter plane for assumed values of constrained quantities². The parameter space is defined by the plane, $E_0 - \lambda$, where E_0 is the amplitude of the accelerating rf field and λ is the rf wavelength. Figures 4-6 show the results of this study at 0.5 TeV, 1.0 TeV, and 2.0 TeV per linac, respectively, for the input parameters given in Table 1, which correspond to the I.P. operating windows found above. The curves include the effects of longitudinal wake fields, and assume that the bunch is displaced from the peak of the rf wave to minimize its energy spread.

TABLE 1

QUANTITY	Fig. 4	Fig. 5	Fig. 6
Energy [TeV]	0.5	1.0	2.0
Average Beam Power [MW]	0.5	1.0	2.0
Luminosity [$\text{m}^{-2}\cdot\text{s}^{-1}$]	1037	4×10^{27}	4×10^{27}
Disruption Parameter	3.0	3.0	3.0
Beamstrahlung Loss	0.3	0.3	0.3
Accelerator Length [km]	≥ 6.0	≥ 12.0	≥ 30.0
Average AC Power [MW]	≤ 50 .	≤ 100 .	≤ 250 .
Pk. RF Power Per Feed [MW]	≤ 500 .	≤ 500 .	≤ 500 .
Energy Spread	$\leq .01$	$\leq .01$	$\leq .01$
$\sigma_x =$ Bunch Length [mm]	0.31	0.15	0.31
$N =$ Number per Bunch	4.2×10^9	6.5×10^8	6.5×10^8
$b =$ Bunches per RF Pulse	10	20	20
Group Velocity/c	.06	.06	.06
Iris Aperture/SLAC Iris	1.315	1.315	1.315
RF Efficiency	0.29	0.29	0.29
Structure Efficiency	0.59	0.59	0.59

* Quantities specified per linac where appropriate.

The inequalities (in italics) represent the constrained values in the allowed region.

In all of the figures the electrical breakdown curve does not constitute a limit on performance. The limit on E_0 is ultimately set by the amount of peak rf or average ac power that one is willing (or able) to provide. Figure 4 shows that the 0.5 TeV/linac case is limited by both peak rf and average ac power at different values of λ . The higher energy cases (Figures 5 and 6) show E_0 limited only by average ac power for the constraint values shown on the curves.

The curve for peak rf power per feed is the same on all three figures, since it depends only on the accelerator structure parameters.

The average ac power curve is computed from the beam power and the total accelerator efficiency. Since the rf efficiency and the structure efficiency are specified (cf. Table 1), the ac power simply scales as the average beam power divided by the beam efficiency, or $P_{AC} \propto P_b E_0 \lambda^2 / bN$. The ac power contour, therefore, is simply $E_0 \lambda^2 = \text{constant}$. The essential point is that

as P_b increases and N decreases as a result of raising the energy and the luminosity, the ac power required for a given E_0 and λ increases. To offset this effect, the number of bunches per rf pulse (b) has been increased from 10 to 20 for the 1.0 and 2.0 TeV linac designs. Even so, the operating window decreases in spite of our having relaxed the constraint from 50 MW/linac at 0.5 TeV to 250 MW/linac at 2.0 TeV.

The energy spread curve is determined by the bunch length, σ_x , which scales as the beam power divided by the luminosity. The 1.0 TeV case, therefore, has the smallest σ_x , and consequently is not constrained by the requirement of $\leq 1\%$ energy spread over the range of λ covered in Figure 5. At 0.5 TeV and 2.0 TeV, the 1% energy spread constraint sets one of the limiting conditions on the plot. At 2.0 TeV, this constraint essentially closes the operating window.

The linac length curve is a measure of the average accelerating gradient. For the 0.5 and 1.0 TeV cases, the gradient has been held to 83 MeV/m, while the gradient for the 2.0 TeV case has been relaxed to 67 MeV/m to provide an operating window.

The effects of transverse wake fields have not been treated explicitly in these calculations, but have been studied separately,¹⁻² and lead to tolerances in the 1μ range for injection offset and cavity alignment, and $\leq 0.1 \mu$ for rms magnet alignment. New techniques, such as BNS damping and rf focusing, appear promising for improving these tolerances.

References

1. A. Mondelli, D. Chernin, V. Granatstein, P. Latham, W. Lawson, and M. Reiser, RF Frequency Scaling and Gyroklystron Sources for Linear Supercolliders, in Frontiers of Particle Beams (Proc. S. Padre Is., Texas, 1986, Lecture Notes in Physics No. 296, M. Month and S. Turner, ed., Springer-Verlag, New York, c. 1988), p. 533.
2. D. Chernin and A. Mondelli, Design Constraints for e+e- Linear Supercolliders, Plasma Technology Notes PTN88-02 (Plasma Technology Division, SAIC, Mc Lean, Virginia, 1988); submitted to Particle Accelerators.
3. P.B. Wilson, Proc. 1987 Part. Accel. Conf. (IEEE Catalogue No. 87CH2387-9, 1987), Vol. 1, p. 53.

Acknowledgement

The authors gratefully acknowledge their collaboration with Martin Reiser and Victor Granatstein at the University of Maryland, and the support of the Department of Energy through Contract Number DEAC05-85ER40216.

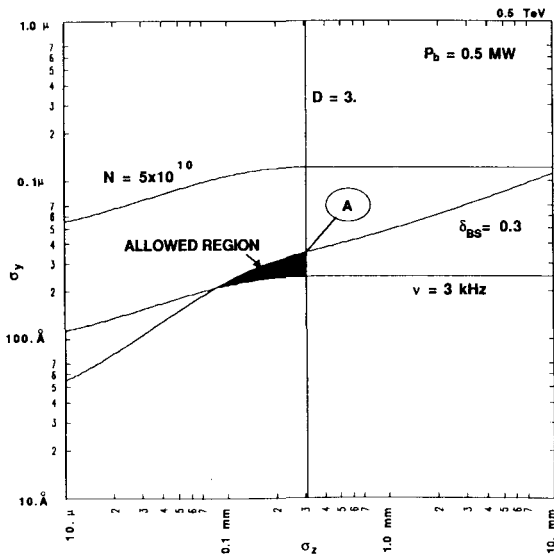


Figure 1: $\sigma_z - \sigma_y$ plane for 0.5×0.5 TeV collider ($P_b = 0.5$ MW)

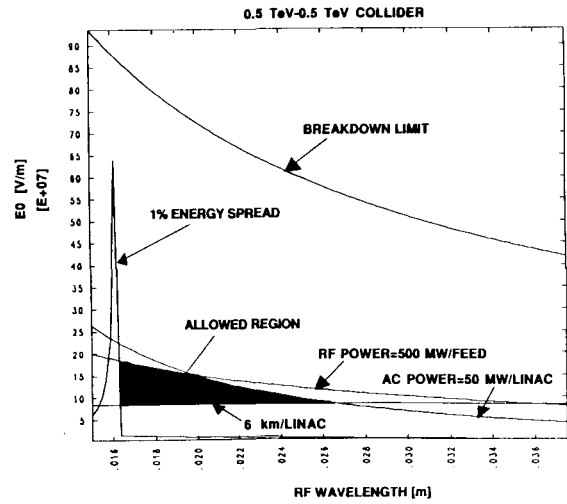


Figure 4: $\lambda - E_0$ plane for 0.5 TeV linac

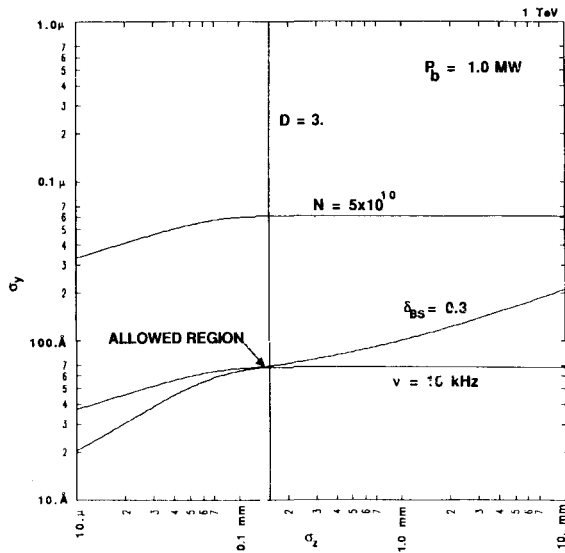


Figure 2: $\sigma_z - \sigma_y$ plane for 1×1 TeV collider ($P_b = 1.0$ MW)

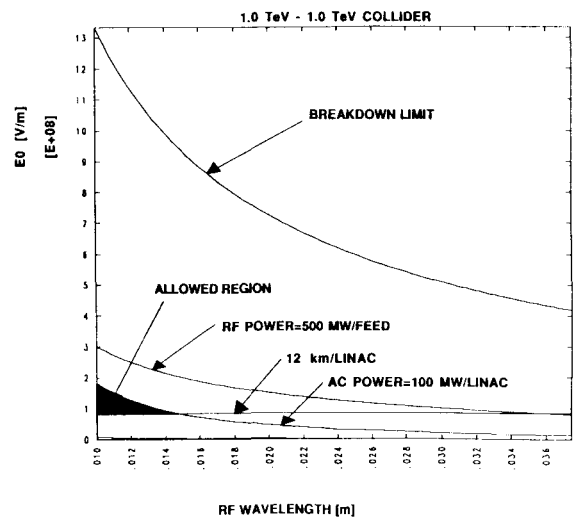


Figure 5: $\lambda - E_0$ plane for 1.0 TeV linac

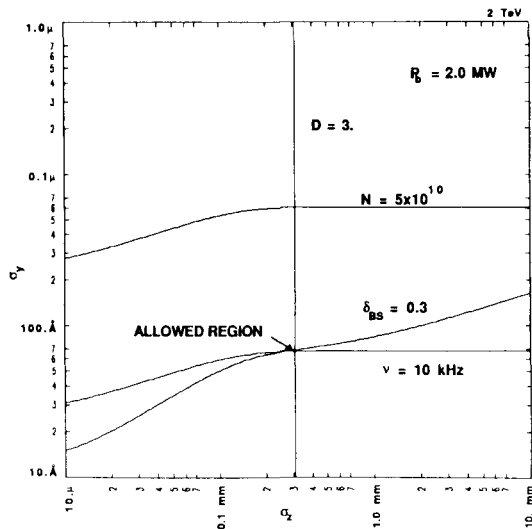


Figure 3: $\sigma_z - \sigma_y$ plane for 2×2 TeV collider ($P_b = 2.0$ MW)

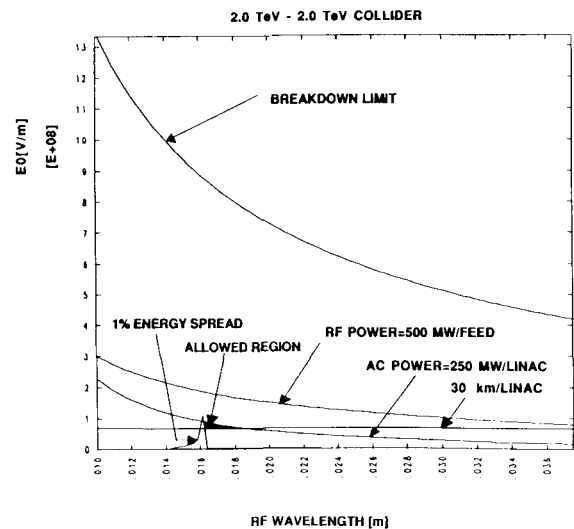


Figure 6: $\lambda - E_0$ plane for 2.0 TeV linac